A Positive Pressure Jamming Based Variable Stiffness Structure and its Application on Wearable Robots

Tianxin Liu, Haisheng Xia, Dae-Young Lee, Amir Firouzeh, Yong-Lae Park, and Kyu-Jin Cho

***Abstract*—Variable stiffness mechanisms establish a bridge between rigid, precise robots and soft, compliant robots. In certain applications it is necessary to exert high forces while having compliance, such as in wearable robots, high payload soft grippers, and manipulators. Negative pressure based jamming approaches have been widely used to tune variable stiffness. However, this variation of stiffness and strength is limited to negative one atmospheric pressure. To enable a wider pressure range which potentially enable wider stiffness range, we proposed a Positive Pressure Jamming (PPJ) approach. The PPJ is fabricated by embedding a pneumatic actuator inside a cylindrical non-stretchable fabric sleeve which contains granules. Pressurizing air into the pneumatic actuator will jam the granules, thus stiffening the soft body. To add degrees of freedom for the PPJ, we place a pair of friction pads in parallel between two PPJ units which act as a self-locking revolute joint. Both the PPJs and self-locking joint can be stiffened at the same time thus enabling the structure to be jammed in multiple configurations. Experiments showed that approximately six-fold stiffness increment (0.69N/mm to 4.02N/mm) could be achieved by our PPJ when input pressure is changed from 68 kPa to 172 kPa with exerted force ranges from 4N to 23N. Furthermore, we apply the proposed PPJ method into limb support devices, demonstrating a promising potential that PPJ has in wearable robot field.**

***Index Terms*—Wearable robotics, mechanism design, stiffness variation, positive pressure jamming.**

I. Introduction

SOFT robots, known as new types of robots which consist of deformable material, demonstrate their unique ability to be highly compliant and adaptable to complex environment [1]. The growing field of soft robotics usually draws inspiration from soft creatures in nature such as octopus, earthworms, or even human vertebra and muscles [2]. Recently, one of the emerging topics related to soft robot is the variability of compliance or stiffness [3], [4]. This online stiffness transition capability in soft robots enables the stiffness of a structure to be tuned as desired, thus broaden their application scope. Such merit of being able to sustain a relatively high payload (in the relative stiff state) while preserving compliance is largely desired in human interactive robots for safety concern [5].

During the past few decades, researchers have investigated a number of novel variable stiffness mechanisms. In general, approaches to stiffen a soft robot can be categorized into two groups, active [6] and semi-active [7], depending on the stiffening principle. Active stiffening approaches use an active actuator to directly generate a resisting force to antagonize external load. For instance, researchers utilized Shape Memory Alloy (SMA) wire to wove in open rectangle loops, which connected with a fixing disc and a movable disc to form a variable stiffness linear actuator [8]. Similarly, applying voltage on two connected and pre-strained Electroactive Polymers (EAPs) could also alter the stiffness of the whole structure [3], [6]. Another group named semi-active variable stiffness technique is achieved by changing the elasticity property of materials, which indirectly alters the stiffness of a structure, such as Low Melting Point Material (LMPM), Electrorheological or Magnetorheological Materials (ERM, MRM) [3]. The above-mentioned methods generally exhibit good performance in stiffness variation, nevertheless, they have some drawbacks like expensive material (EAPs, SMA), sophisticated fabrication process (ERM, MRM), or low energy efficiency (LMPM).

Jamming approach [9]–[11], being classified into the semi-active stiffening group, has raised much attention among researchers since it can be a robust, low-cost and easy customized way to make reconfigurable variable stiffness robots [12]. In granular jamming, a cluster of independent particulate material has the characteristic of increasing viscosity when densified by external pressure, which can change their overall behavior from fluid to solid. Many works related to jamming adopted granules or pieces of layers as the medium to create a series of applications-soft manipulator [12][13], drone landing damper [14], soft robot hand [15], arm support [16], and minimally invasive surgery device [17]. Li et al. [18] developed a passive jamming gripper based on positive pressure with the granules at the top layer of the actuator compressed by the bending of the actuator. Though their design enlarged the stiffness variation significantly, the stiffness variation and gripper's bending motion are coupled. Sridar et al. [27] utilized fluid to jam granules for bearing axial compression load in their variable stiffness exoskeleton or eliminate bowing problem but it cannot conform

Manuscript received March 14, 2021; accepted June 28, 2021. Date of publication July 14, 2021; date of current version August 23, 2021. This letter was recommended for publication by Associate Editor C. Della Santina and Editor C. Gosselin upon evaluation of the reviewers' comments. This work was supported by the National Research Foundation of Korea (NRF) Grant funded by the Korean Government (MSIT) (Grant No. NRF-2016R1A5A1938472). *(Tianxin Liu and Haisheng Xia are co-first authors.) (Corresponding author: Kyu-jin Cho.)*

Tianxin Liu, Amir Firouzeh, and Kyu-Jin Cho are with the Soft Robotics Research Center, BioRobotics Laboratory, Department of Mechanical Engineering, Institute of Advanced Machines and Design (IAMD), Institute of Engineering Research, Seoul National University, Seoul 08826, South Korea (e-mail: tliuao@connect.ust.hk; amir.firouzeh@epfl.ch; kjcho@snu.ac.kr).

Haisheng Xia is with the Department of Automation, University of Science and Technology of China, Hefei, Anhui 230026, China (e-mail: hsxia@ustc.edu.cn).

Dae-Young Lee is with the Microrobotics Laboratory, Materials Science & Mechanical Engineering, Harvard University, Cambridge, MA 02138 USA (e-mail: dylee@seas.harvard.edu).

Yong-Lae Park is with the Department of Mechanical Engineering, Soft Robotics Research Center (SRRC), Institute of Advanced Machines and Design (IAMD), the Institute of Engineering Research, Seoul National University, Seoul 08826, South Korea (e-mail: ylpark@snu.ac.kr).

Digital Object Identifier 10.1109/LRA.2021.3097255

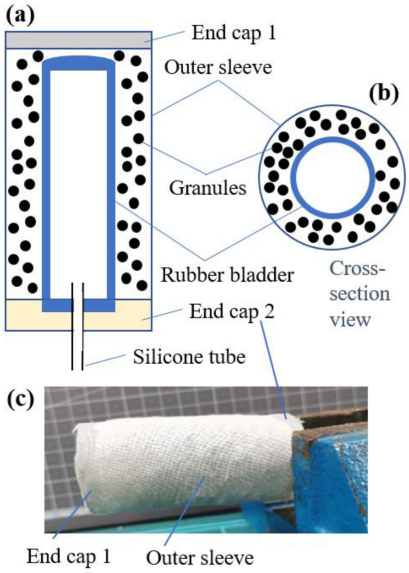

Fig. 1. (a) Structure of a single PPJ unit, the rubber bladder and silicon tube form a soft actuator, which can squeeze the granules and stiffen the PPJ unit. (b) Cross-section view of the PPJ unit. (c) Prototype of a single PPJ with a diameter of 26mm and length of 50mm.

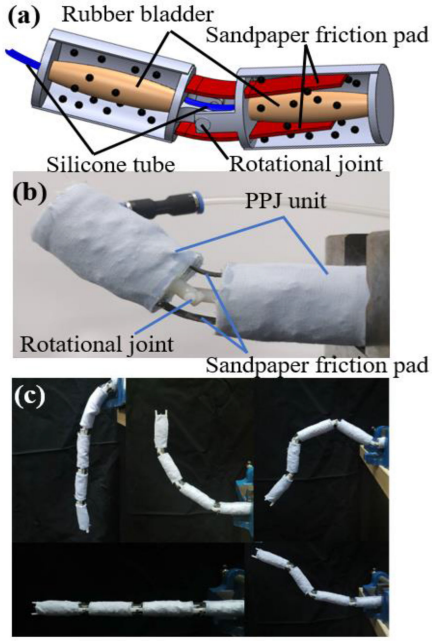

Fig. 2. (a) 3D modeling of two PPJ units with a self-locking-joint formed by sandpaper friction pads and rotation joint. (b) Prototype of two PPJ units with a self-locking-joint. (c) Prototype of multiple PPJ units connected by self-locking-joints, with the top-left in soft condition and the rest in stiffen condition.

to different shapes. We propose a variable stiffness structure that can be directly stiffened by Positive Pressure Jamming (PPJ) and varying the stiffness does not affect the actuator geometry. Specifically, we squeeze air into a rubber bladder which is embedded in the granular medium as a source to provide external force for jamming. Detailed design can be seen in the next chapter. Based on the nature of positive pressure, this design would potentially have several benefits in the following aspects:

(1 Wider pressure limit. The maximum negative pressure in theory is negative one atmosphere relative pressure, while positive pressure could exceed positive ten atmospheres relative pressure with ease. Thus, with a wider pressure limits for PPJ, the force applied on the granular materials could be higher [12].

(2 Easier to be portable. To achieve the same amount of relative pressure, PPJ could use smaller pump than negative pressure jamming application, which is usually heavy and bulky [19].

The rest of our paper is organized as follows: Section II describes detailed design of PPJ and fabrication process. After that, several experiments and analysis are presented in Section III. Section IV demonstrates an application of PPJ in the wearable robot field. Finally, an overall summary is drawn in Section V.

II. Design and Fabrication

A. Concept Design

The proposed PPJ structure consists of a soft rubber bladder, granules, a fabric outer sleeve, two end caps and a silicon tube as shown in Fig. 1a. The rubber bladder connecting with the silicon tube serves as a soft actuator that can be inflated when squeezing positive pressure into the rubber bladder. The non-stretchable outer fabric sleeve together with two end caps composes a cylindrical shape. In between the outer fabric sleeve and inner rubber bladder are granular materials. To reach a relative stiff state, air is squeezed into the rubber bladder. The volume expansion of the rubber bladder could transmit force to granules, and in the meantime, the outer fabric sleeve constrains the volume of the whole structure, seen in Fig. 1b cross-section view. In this way, granular materials within the outer fabric sleeve would be squeezed by the inflated inner rubber bladder. Thus, its stiffness can be dramatically enhanced. Inflatable rubber bladder placed concentric to the outer cylinder to active jamming when pressurized. When the rubber bladder is deflated, the PPJ structure again recovers to a soft state, which can be easily bent, twisted, or compressed.

One unit of the jamming structure merely provides cylindrical shape configurations under the stiffened state. To further explore the application scope and improve the compliance, we design a self-locking mechanism and utilize multiple jamming units in serial that can be stiffened in multiple shapes (Fig. 2). We add a pair of friction pads and fix one end of the friction pad to the end cap and the other end of friction pad penetrate into a PPJ chamber through small square holes on the end cap (Fig. 2a). Using this structure, when the rubber bladder is inflated, not only it compresses the granules, but also it compresses the friction pads. If an external force is applied on the joint causing a torque, the pair of opposite friction force on two friction pads could produce a reverse torque to balance that. As a result, one can rotate the joint to any angle and lock the joint at that angle by pressurizing the rubber bladder. In this case, shape locking and stiffening occur simultaneously and are achieved by a single actuator. Fig. 2b displays a prototype of this idea with two PPJ units as links which are connected by friction pads and a rotational joint. Rotation angles range from -50 degrees to 50 degrees can be achieved and locked by this device. In Fig. 2c, we demonstrate more configurations by employing more PPJ units. Fig. 2c top-left shows the natural shape when there is

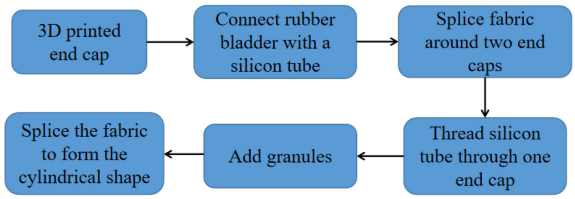

Fig. 3. Fabrication process.

no additional air pressure. In the rest sub-figures of Fig. 2c, we manually change the shape and then pressurize air into the actuator. The shape can be preserved by stiffening for all the cases.

B. Fabrication

The Fabrication process is shown in Fig. 3. The rubber bladder can be obtained by molding process with silicon or just use commercially available rubber bladder (latex balloon, long type). We connect the rubber bladder with a tube by adding adhesive (LOCTITE 908570 Silicone Sealant) between the outer surface of the tube and hole on the rubber bladder, and fasten the connection with sewing thread. The outer fabric sleeve is made of a common single-ply non-stretchable fabric. We wrap it around the 3D printed end cap and use UHU all-purpose glue for adhesion. Before the outer fabric sleeve is completely spliced, we add granules into this chamber. Shape Memory Polymer (SMP, MM type, SMP Technologies. Inc.) granular are selected due to the reason that the high rigidity of SMP granular can minimize the effects of deformations of the media materials on stiffness performance. Each SMP granular roughly has a size of 2mm$\times$2mm$\times$3mm in cuboid shape. For the self-locking jamming system, the fabrication process is similar to the single PPJ unit except for adding rotational joints, two pieces of friction pads and a silicon tube connecting rubber bladders in the neighbor chambers. The friction pad is fixed on the end cap of one PPJ and goes into the neighbor PPJ (Fig. 2). And the friction pad is fabricated by a lamination process with three layers, of which the top and bottom layers are sandpaper and the middle layer is thermoplastic polyurethanes. A cylindrical shape PPJ module (Fig. 1c) in the size of 26 mm diameter and 50 mm length was fabricated for the following test.

III. Experiments and Analysis

For evaluation and investigation of the characteristics of the proposed PPJ structure, several experiments based on cantilever bending test [20] have been conducted to compare the stiffness (Fig. 4). A tensile test system (UNITECH, RB302 Microload) and load cells (DACELL) were utilized in our experiments for force measurement. The general procedure of cantilever bending tests is as follows. Firstly, fix one end of the PPJ on the clamp and pressurize air into it to reach a stiff state. Then, adjust the position of the specimen so that its endpoint contacts the load cell. After that, start the test program to let the load cell push the specimen downwards to around 11 mm at the speed of 20 mm per minute and return with the same speed. Force versus displacement data can be automatically recorded on a computer with a data acquisition card. Our experiments mainly include verification for stiffness variation and investigation of some parameters which affect the jamming.

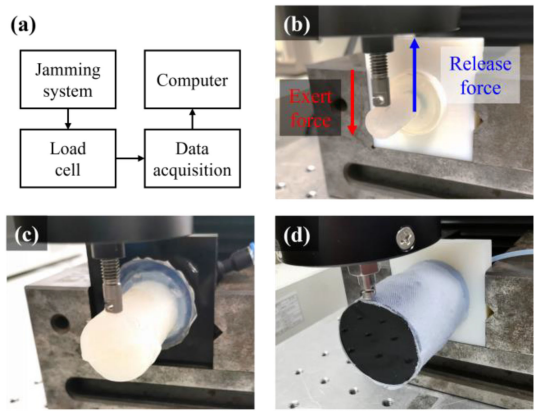

Fig. 4. Test on 3 types of specimens. (a) Experiment set up. (b) Rubber bladder. (c) Negative pressure jamming unit. (d) Proposed PPJ structure.

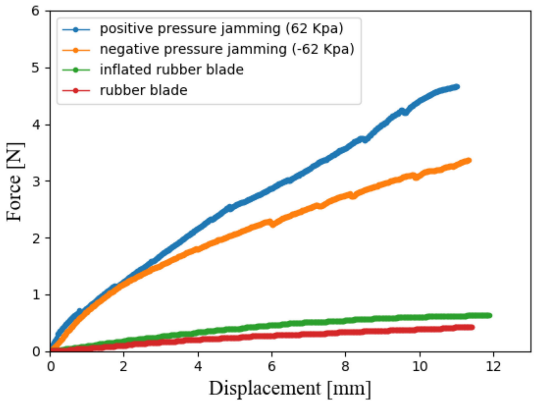

Fig. 5. Resisting force versus displacement for different types of test specimen.

A. Stiffness Characterizations

The objective of this experiment is to verify the stiffness and strength increment achieved by granules jammed with positive pressure. For comparison purpose, another same size rubber bladder (Fig. 4b), a negative pressure jamming module (Fig. 4c) with the same size and same granules volume fraction were fabricated as well. We independently conduct the cantilever bending tests on the rubber bladder without and with additional pressure (62 kPa) as baseline, on the PPJ module with additional pressure (62 kPa), and on the fabricated negative pressure jamming module with negative pressure (-62 kPa, which is 62 kPa below atmospheric pressure). As it is shown in Fig. 5, only inflating the rubber bladder can hardly contribute to the stiffness enhancement. When the pressure is transmitted to peripheral granules to incur jamming phenomenon, the stiffness can be dramatically increased. The negative pressure jamming, shown in the brown line, roughly has the same stiffness as PPJ in the first few steps of displacement. It tends to saturate at a maximum force and has large hysteresis [21]. In contrast, PPJ structure is less obvious in plastic deformation under the same amount of displacement as the inner rubber bladder increases its elasticity.

During the jamming process, squeezing high-pressure air into the inner air bladder can also contribute to the stiffness enhancement. Nagase et al. [22] reported compressed air-based method for variable stiffness with fiber reinforcement pneumatic actuator. Therefore, to compare the stiffness variation caused by

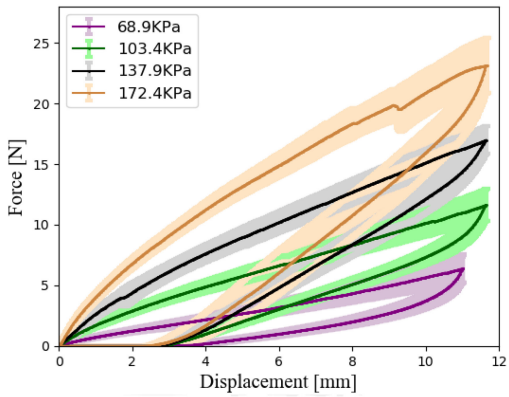

Fig. 6. Resisting force versus displacement for PPJ under four different pressure levels. The mean values of 8 times repeated tests are represented by curve lines and the light shaded parts around the curves show the variation with 95% confidence interval.

compressed air and granular jamming, we conduct an additional group of tests. The input pressure is set to 103 kPa for an air sealing cylindrical airbag and our PPJ specimen, and the outer diameter of those two are the same. We find that the granular jamming has 40% higher stiffness than the compressed air specimen which indicates granular jamming plays a principal role in stiffness enhancement.

B. Pressure Modulation

Our proposed PPJ structure takes pressure as an input and outputs stiffness variation. To investigate the relationship between the input pressure and output stiffness, four different pressure levels: 69 kPa, 103 kPa, 138 kPa, 172 kPa (relative pressure) were set up in a PPJ specimen, and cantilever bending tests were adopted again. We use the same PPJ specimen as shown in Fig. 4d. The result is shown in Fig. 6. It can be seen that for the same specimen, the higher input pressure leads to higher stiffness. We utilize the measured force value of the first 1mm displacement of the specimen to calculate the stiffness, which is during the elastic deforming period where small deformation and payload in-situ is expected. The results for the 4 increasing levels of pressure are 0.69 N/mm, 1.72 N/mm, 2.75 N/mm, and 4.02 N/mm, respectively. And the corresponding R^2 value for the fitting are 0.992, 0.995, 0.994, and 0.993, respectively.

The data indicates that the stiffness is approximately proportional to the input air pressure. Different from layer jamming, where maximum pressure is limited to negative one atmospheric pressure and the stiffness is usually dependent on the number of layers, the stiffness of PPJ can be tuned by input pressure [23]. This can be explained by that there is no slip between two layers when the shear force is less than the limit of friction force. However, for the granular jamming, relative displacement between granules occurs at the beginning stage so that the friction force (affected by pressure) contributes to the overall stiffness [23].

C. Characterization Vs Geometry

The previous section shows the stiffness of the PPJ structure can be tuned by changing input pressure level, while in this section, we will investigate design parameters that affect the jamming performance under the same pressure level. Factors

TABLE I
EQUIVALENT YOUNG'S MODULUS WITH DIAMETER

Equivalent Young's modulus (MPa)		Outer Diameter			
		26 cm	29 cm	32 cm	35 cm
Inner Diameter	10 cm	8.6	5.2	2.9	2.6
	15 cm	11.7	5.8	4.2	3.1

such as the material of granules, the volume fraction of granules [24], type of outer fabric, and size of the PPJ structure can affect the stiffness of the PPJ when inflated. Since selecting strong and non-stretchable fabric (higher binding force) and soft inner rubber bladder (consume less elastic energy) is preferred and intuitive for PPJ design, we simply only investigate the size parameter. Outer diameter (D) of fabric sleeve and inner diameter (d) of rubber bladder are the two key parameters. We manufactured 8 specimens at four different D parameters (26 mm, 29 mm, 32 mm, 35 mm) with two different d parameters (10mm and 15mm) for the cantilever bending tests under one atmosphere relative pressure. Nearly a hundred percent granules volume fraction (defined in [24]) is adopted to eliminate the effect by rubber bladder morphing. We calculate the stiffness and equivalent Young's modulus (bending elastic modulus which represents how strong the jammed granules can resist to bending deformation) based on the first 1 mm displacements during the elastic deforming period, where small deformation and payload in-situ is expected. Results of 8 repeated tests are shown in Fig. 7.

For both small and large inner rubber bladders, the stiffness of PPJ increases with the increment of outer diameter because the moment of inertia of cross-section enlarges as well. However, the equivalent Young's modulus demonstrates a reverse trend. This phenomenon could possibly due to that for the specimen with a larger outer diameter, it contains more layers of granules and the force transmit from inner rubber bladder to outer layers deteriorates as outer layers have more granules which make the outer layers being compressed less firmly as compared to inner layers of granules. Comparing the result of the same outer diameter with different inner diameters, it is noticeable that the equivalent Young's modulus of PPJ were larger with larger inner rubber bladder diameter (Table I), which could indicate that PPJ with bigger inner rubber bladder was compressed more firmly than PPJ with smaller inner rubber bladder.

A few simple formulas may better explain this phenomenon. Consider jammed granules in the PPJ as a beam with a ring shape cross-section (Fig. 1b). We assume the specimen is fully jammed by a large enough pressure and it is under tiny deformation (no slip between granules), the cantilever bending stiffness K can be expressed as

$$K = 3EI/L^3 \tag{1}$$

where E is equivalent Young's modulus, I is the moment of inertia of cross-section. L is the total length of the PPJ structure. For the ring shape cross-section, I is expressed by

$$I = \pi\left(D^4 - d^4\right)/64 \tag{2}$$

Assume that granules are evenly distributed in the chamber and ignore other factors like fabric material, coefficient of friction (being treated as constants), we define the equivalent Young's modulus of the PPJ structure based on the experimental results in Fig. 7. We find it possibly proportional to $1/(D^2-d^2)$ as

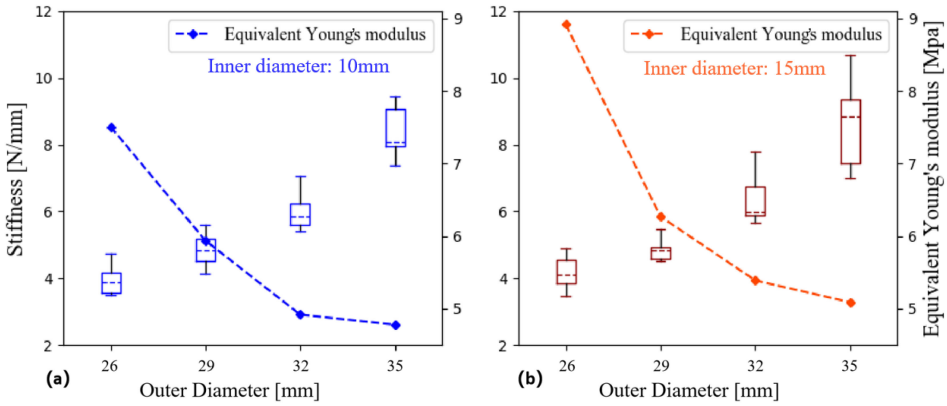

Fig. 7. Influence of size of inner diameter and outer diameter on stiffness (box plot) and equivalent Young's modulus (dot line). (a) PPJ unit with 10 mm inner rubber bladder diameter. (b) PPJ unit with 15 mm inner rubber bladder diameter.

the equivalent Young's modulus is related to the average force exert on the granules, and higher average force would jam each granule firmer thus increase the stiffness. The cross-section of our PPJ is a ring shape (Fig. 1), when the total force exerted on the granules is F_t, the average force in one cross section area can be expressed as $F_{average} = 4Ft/\pi(D^2\text{-}d^2)$, thus the equivalent Young's modulus is possibly proportional to $1/(D^2\text{-}d^2)$. Therefore, equivalent Young's modulus of PPJ can be expressed by (3), and C is a coefficient (with unit) that is decided by other factors like pressure and material, which could be fixed as a dimensional constant here.

$$E = \mathrm{C}/\left(D^2 - d^2\right) \tag{3}$$

Combining (1)(2)(3), the stiffness can be expressed as a function of D and d.

$$K = 3\pi C\left(D^2 + d^2\right)/64L^3 \tag{4}$$

This function shows that both increments of the D and d can benefit the stiffness as a larger D means a larger moment of inertia and larger d means higher equivalent Young's modulus. Nevertheless, what makes the PPJ structure more meaningful than stiffness is the efficiency of jamming which is defined as stiffness per unit mass, shown in (5).

$$\mathrm{K/mass} = \frac{3C\left(D^2 + d^2\right)}{16L^4\rho_0\left(D^2 - d^2\right)} \tag{5}$$

where ρ_0 is the measured density of granules in a certain space and the first term in this equation is a constant. Equation (5) is depicted in Fig. 8 and we set $D = 26$ mm and $d = 10$ mm as a baseline. So, each value calculated by equation (5) is relative value with respect to baseline with the unit of times. Fig. 8 illustrates that when D and d get closer to each other, the PPJ module can reach a global optimal jamming efficiency.

D. Stiffness of two PPJ Links With a Self-Locking Joint

In this experiment, we conducted a cantilever bending test on our proposed compliant jamming structure, a self-locking joint connecting two PPJ links. The diameter (D) and length (L) of one PPJ unit are 26 mm and 50 mm respectively which are the same as the specimen in Fig. 4d. The rotational joint consists a hinge joint and a pair of friction pads, and measures 15 mm (l) when the two PPJ units are in a straight line.

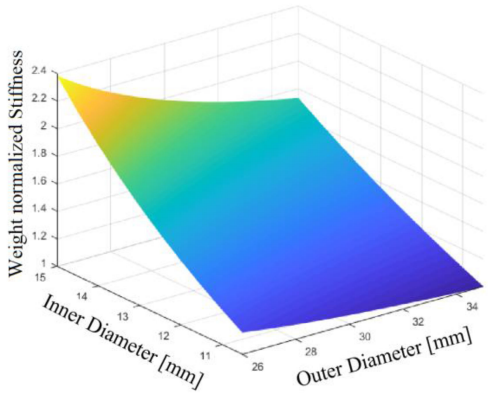

Fig. 8. Computational result of stiffness over weight ratio versus inner diameter and outer diameter.

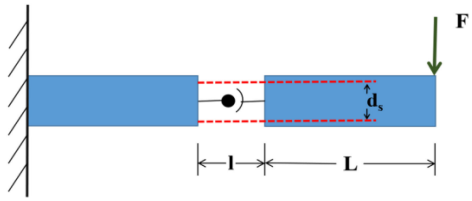

Fig. 9. Diagram of the cantilever bending test for two PPJ links and a self-locking joint. The red dotted lines represent a pair of friction pads.

The general diagram for the cantilever bending test is depicted in Fig. 9 and the reaction force versus displacement is recorded. Fig. 10 shows the experimental result for three different levels of input pressure conditions. It can be seen that the structure undergoes two stages: first (within 2 mm displacement), the external force (F) only causes bending deformation of the PPJ links since the joint is locked by the friction pads. Second (after 2 mm displacement), the torque at the joint position generated by the external force exceeds the limit of the self-locking joint and friction pads start to slide. In this stage, the reaction force gradually stabilizes while the deformation of the specimen continues increasing. The critical point force (F_c) for the self-locking joint starting to rotate can be represented by torque balance in (6).

$$F_c\left(L + l/2\right) = PS\mu d_s \tag{6}$$

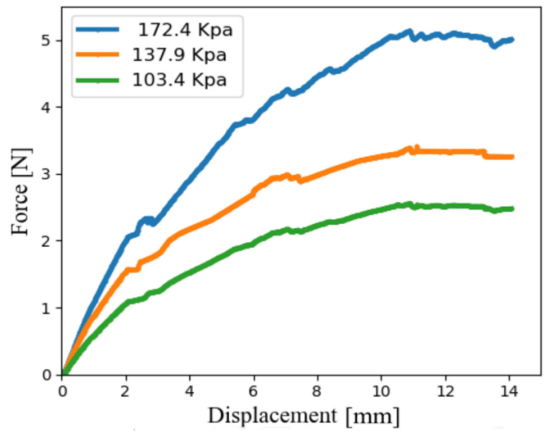

Fig. 10. Force-displacement curve for the cantilever bending test of the self-locking joint with PPJ links.

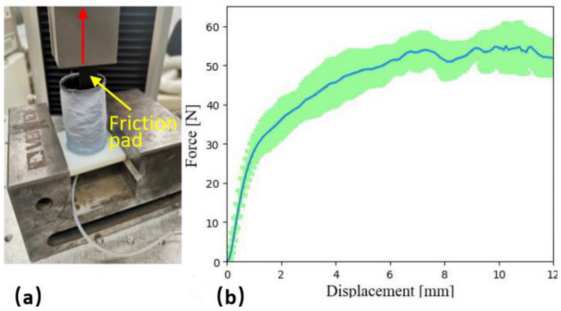

Fig. 11. Test of friction force. (a) Experimental setup, a PPJ unit is fixed by a fixture and a sandpaper friction pad is inserted in the PPJ through a hole. A clamp with a load cell pulls the sandpaper friction pad out of the PPJ unit. (b) Force versus displacement of the sandpaper friction pad. Blue line is the average value of 6 tests and light green shade is variation with 95% confidence interval.

where P is input pressure, S is the total contact area between friction pad and granules, μ is the coefficient of maximum static force, and d_s is the distance between two friction pads. We ignore the bending angle when calculating torque generated by external force since the angle is very small. Thus, the stiffness of this two-link-one-joint structure can be represented by:

$$k \approx \begin{cases} k_{links} & , F <= \mathrm{F_c} \\ 0 & , F > \mathrm{F_c} \end{cases} \tag{7}$$

When the external force is less than the critical point, the stiffness of the whole structure is close to the stiffness of two links connected in serial. However, the joint loses its efficiency when the external force is larger than the critical point.

Since the friction force directly leads to the shape locking at any arbitrary rotation angle within the range, we measure the friction force instead of rotation stiffness. Fig. 11 shows the sliding friction force when a piece of sandpaper friction pad is pulled out of the PPJ chamber under 137 kPa input pressure, from the experiment we could estimate that the coefficient μ is 1.09. It can be seen that the friction pad could support 30N before the locking will fail, indicating the self-locking joint torque limit of 0.6Nm.

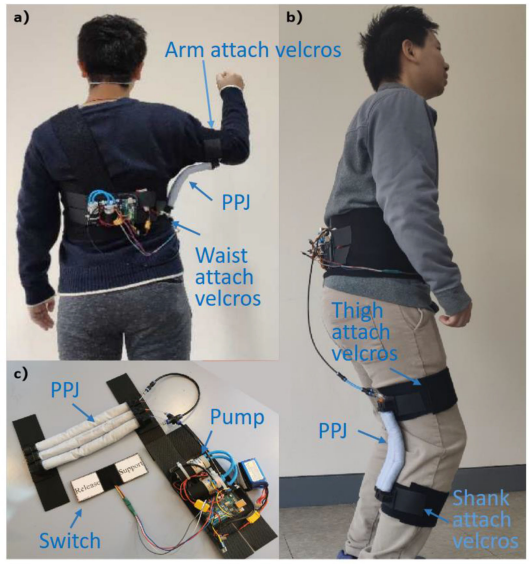

Fig. 12. (a) and (b) Wearable device consisting PPJ structure to help supporting the arm and the leg. (c) Electromechanical structure.

IV. Limb Support Applications

Most commercially available limb support devices for force assistance purpose adopt rigid material to endure high payload. And for rehabilitation purpose, Hashimoto et al. [25] designed an upper limb support device with pneumatic cylinder to support patients' arm motion. For those rigid-frame-based limb support devices, conformability and safety might be big issues. On the contrary, variable stiffness mechanism made from soft material is preferable for wearable device as its stiffness can be tuned to a proper value for functionality while ensuring safety. It is also easy to use since people can simply tune it to soft state rather than take off it when the limb does not need support. O'Neill et al. [26] developed a soft wearable robot for the shoulder support with textile pneumatic actuators, which generated a force of 17 N at 70 kPa when bending at 90 degrees. Nevertheless, PPJ with granule has a potential to make the support more stable as the interlocking between each granule has damping effect. Here, we demonstrate a PPJ method based limb support device shown in Fig. 12. The system mainly consists of two motor pumps in serial, a solenoid valve, switches, three PPJ in parallel, an Arduino controller, and velcros for anchoring. For arm support, the three links are connected in parallel and one end is attached to the waist of body and another end is attached to the arm. For leg support, one end is attached to the thigh and the other end to the shank. Take the arm support for example, when there is no additional air pressure in the PPJ units, users can freely raise up or low down their arms. Adjusting arm to a desired position and activating the motor pumps, the three PPJ units become stiffened and have a tendency to transform from curved shape to straight cylindrical shape thus generating adequate force to support the arm. Release air pressure, the PPJ units return to soft state again. The whole system (Fig. 12c) weighs around 400 grams and each PPJ unit measures 200 mm in length and 20 mm in diameter. Each motor pump can generate roughly 1 atmospheric pressure. In our application, we connect two motor pumps in serial to achieve larger pressure.

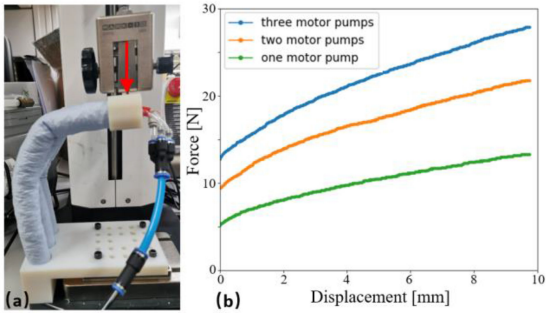

Fig. 13. (a) Experimental setup. The specimen is pre-bended to 90 degrees. One end is fixed on the fixture and the other end is attached to the load cell head. (b) Experiment result of force versus displacement for the three paralleled PPJ structure driven by different number of motor pumps.

To verify and evaluate the performance of the proposed limb support device, several stiffness tests have been conducted (Fig. 13a). We fix one end of PPJ units on the fixture and bend the soft state links to 90 degrees. Align the center of the load cell head to the other endpoint of PPJ units. Then we activate the motor pump to stiffen the links. After they are fully stiffened, control the force measuring head to move down. Force versus displacement curve is recorded as shown in Fig. 13b. The initial force measured for using one, two and three motor pumps (input pressure approximately 100.5 kPa, 195.6kPa, 290.1kPa, respectively) in serial are 5.2 N, 9.4 N, and 12.8 N respectively while the corresponding force increments for 10 mm displacement are 8.1 N, 12.4 N, and 15.1 N. This experiment indicates that the PPJ based device can generate assisting force to help limbs support, which withstand part of the force needed for certain postures. The force generated in our study is slightly smaller than O'Neill et al. [26], possibly due to that they design special structure to divide the pneumatic actuator into multiple champers thus increase the stiffness. We should also consider adding partitions to the PPJ to explore different potential of increasing stiffness.

V. Conclusion and Future Work

This letter illustrates the concept, design, fabrication, experiment results as well as the characteristic analysis of our proposed PPJ structure. A significant stiffness enhancement can be achieved by our proposed PPJ method. To overcome the inherent drawbacks that the shape of one PPJ unit is confined by the outer sleeve, we developed a self-locking joint mechanism with multiple rotational links for various configurations. Several experiments along with mathematical models related to size parameters can be a guide for design. Finally, we demonstrate a possible application in wearable robot based on the force generation of the PPJ.

One limitation of our proposed PPJ structure is that it cannot have any arbitrary shapes and the stability of jamming performance relies highly on the initial distribution of granules inside the fabric sleeve. The maximal angle one PPJ unit could reach also depends highly on the initial distribution of the granules, as well as the percentage that the granules fill the chamber. To increase flexibility, we designed the self-locking joint. Another limitation is that we use a soft rubber bladder to enable shape forming at atmospheric pressure, which means the air chamber at positive pressure can still be deformed, reducing the jamming effect. Additionally, the self-locking joint mechanism would potentially wear out over time as the sandpaper loses its friction due to abrasion.

In our future work, we should explore using pre-designed outer sleeve to make PPJ structure into other shapes such as torus shape. We may combine different shapes of PPJ structures to form a complex 3D frame for some practical applications such as a frame for a tent. PPJ potentially has faster response time than negative jamming, especially for wearable application, as for pumps with same size, positive pressure pump is usually more powerful than vacuum pump. Though more tests are need to verify state transition time from soft to stiff and from stiff to soft. Future works should explore new materials for the rubber bladder to reduce deformation during the stiffened state, and new materials for the friction pad to increase durability. In addition, we are interested in studying how to stabilize the jamming. For example, divide the inner space area of a jamming unit by adding some partitions with fabric so that the initial distribution of granules can be more even. We hope that this paper can inspire more researches in jamming based variable stiffness field.

References

[1] G. M. Whitesides, "Soft robotics," *Angewandte Chemie Int. Ed.*, vol. 57, no. 16, pp. 4258–4273, 2018.
[2] S. Kim, C. Laschi, and B. Trimmer, "Soft robotics: A bioinspired evolution in robotics," *Trends Biotechnol.*, vol. 31, no. 5, pp. 287–294, 2013.
[3] M. Manti, V. Cacucciolo, and M. Cianchetti, "Stiffening in soft robotics: A review of the state of the art," *IEEE Robot. Autom. Mag.*, vol. 23, no. 3, pp. 93–106, Sep. 2016.
[4] S. P. M. Babu, A. Sadeghi, A. Mondini, and B. Mazzolai, "Antagonistic pneumatic actuators with variable stiffness for soft robotic applications," in *Proc. IEEE Int. Conf. Soft Robot.*, 2019, pp. 283–288.
[5] A. Stilli, L. Grattarola, H. Feldmann, H. A. Wurdemann, and K. Althoefer, "Variable stiffness link (VSL): Toward inherently safe robotic manipulators," in *Proc. IEEE Int. Conf. Robot. Automat.*, 2017, pp. 4971–4976.
[6] R. Pelrine, F. Carpi, D. De Rossi, R. Kornbluh, R. Pelrine, and P. Sommer-Larsen, "Variable stiffness mode: Devices and applications," *Dielectric Elastomers as Electromechanical Transducers: Fundamentals Mater. Devices Models Appl. Emerg. Electroactive Polym. Technol.*, pp. 141–145, 2008.
[7] A. J. Liu and S. R. Nagel, "Nonlinear dynamics: Jamming is not just cool anymore," *Nature*, vol. 396, no. 6706, pp. 21–22, 1998.
[8] D. Nalini, D. J. S. Ruth, and K. Dhanalakshmi, "Design of a variable stiffness actuator using shape memory alloy wire," in *Proc. IEEE 7th Power India Int. Conf.*, 2016, pp. 1–5.
[9] Y. Chen, Y. Li, Y. Li, and Y. Wang, "Stiffening of soft robotic actuators—Jamming approaches," in *Proc. IEEE Int. Conf. Real-Time Comput. Robot.*, 2017, pp. 17–21.
[10] V. Wall, R. Deimel, and O. Brock, "Selective stiffening of soft actuators based on jamming," in *Proc. IEEE Int. Conf. Robot. Automat.*, 2015, pp. 252–257.
[11] P. Jiang, Y. Yang, M. Chen, and Y. Chen, "A variable stiffness gripper based on differential drive particle jamming," *Bioinspiration Biomimetics*, vol. 14, 2019, Art. no. 036009.
[12] N. G. Cheng *et al.*, "Design and analysis of a robust, low-cost, highly articulated manipulator enabled by jamming of granular media," in *Proc. IEEE Int. Conf. Robot. Automat.*, 2012, pp. 4328–4333.
[13] J. R. Amend, E. Brown, N. Rodenberg, H. M. Jaeger, and H. Lipson, "A positive pressure universal gripper based on the jamming of granular material," *IEEE Trans. Robot.*, vol. 28, no. 2, pp. 341–350, Apr. 2012.
[14] Y. S. Narang, A. Degirmenci, J. J. Vlassak, and R. D. Howe, "Transforming the dynamic response of robotic structures and systems through laminar jamming," *IEEE Robot. Autom. Lett.*, vol. 3, no. 2, pp. 688–695, Apr. 2018.
[15] K. Mizushima, T. Oku, Y. Suzuki, T. Tsuji, and T. Watanabe, "Multi-fingered robotic hand based on hybrid mechanism of tendon-driven and jamming transition," in *Proc. IEEE Int. Conf. Soft Robot.*, 2018, pp. 376–381.
[16] S. Hauser, M. Robertson, A. Ijspeert, and J. Paik, "Jammjoint: A variable stiffness device based on granular jamming for wearable joint support," *IEEE Robot. Autom. Lett.*, vol. 2, no. 2, pp. 849–855, Apr. 2017.

[17] M. Cianchetti, T. Ranzani, G. Gerboni, I. De Falco, C. Laschi, and A. Menciassi, "STIFF-FLOP surgical manipulator: Mechanical design and experimental characterization of the single module," in *Proc. IEEE/RSJ Int. Conf. Intell. Robots Syst.*, 2013, pp. 3576–3581.

[18] Y. Li, Y. Chen, Y. Yang, and Y. Wei, "Passive particle jamming and its stiffening of soft robotic grippers," *IEEE Trans. Robot.*, vol. 33, no. 2, pp. 446–455, Apr. 2017.

[19] L. Wang *et al.*, "Controllable and reversible tuning of material rigidity for robot applications," *Mater. Today*, vol. 21, no. 5, pp. 563–576, 2018.

[20] L. Blanc, B. François, A. Delchambre, and P. Lambert, "Granular jamming as controllable stiffness mechanism for endoscopic and catheter applications," in *Proc. Congrès Français de Mécanique*, 2017.

[21] A. Jiang, A. Ataollahi, K. Althoefer, P. Dasgupta, and T. Nanayakkara, "A variable stiffness joint by granular jamming," in *Proc. Int. Des. Eng. Tech. Conf. Comput. Inf. Eng. Conf.*, 2012, vol. 45035, pp. 267–275.

[22] J. Nagase, S. Wakimoto, T. Satoh, N. Saga, and K. Suzumori, "Design of a variable-stiffness robotic hand using pneumatic soft rubber actuators," *Smart Mater. Structures*, vol. 20, no. 10, 2011, Art. no. 105015.

[23] Y. S. Narang, J. J. Vlassak, and R. D. Howe, "Mechanically versatile soft machines through laminar jamming," *Adv. Funct. Mater.*, vol. 28, no. 17, 2018, Art. no. 1707136.

[24] A. Jiang, G. Xynogalas, P. Dasgupta, K. Althoefer, and T. Nanayakkara, "Design of a variable stiffness flexible manipulator with composite granular jamming and membrane coupling," in *Proc. IEEE/RSJ Int. Conf. Intell. Robots Syst.*, 2012, pp. 2922–2927.

[25] Y. Hashimoto, J. Y. Nagase, N. Saga, and T. Satoh, "Development and control of support function for upper limb support device," in *Proc. IEEE Int. Conf. Ind. Technol.*, 2016. pp. 1566–1571.

[26] C. T. O'Neill, N. S. Phipps, L. Cappello, S. Paganoni, and C. J. Walsh, "A soft wearable robot for the shoulder: Design, characterization, and preliminary testing," in *Proc. Int. Conf. Rehabil. Robot.*, 2017, pp. 1672–1678.

[27] S. Sridar, C. J. Majeika, P. Schaffer, M. Bowers, and S. Ueda, A. J. Barth, J. L. Sorrells, J. T. Wu, T. R. Hunt, and M. Popovic, "Hydro muscle-a novel soft fluidic actuator," in *Proc. IEEE Int. Conf. Robot. Autom.* , 2016, pp. 4014–4021.